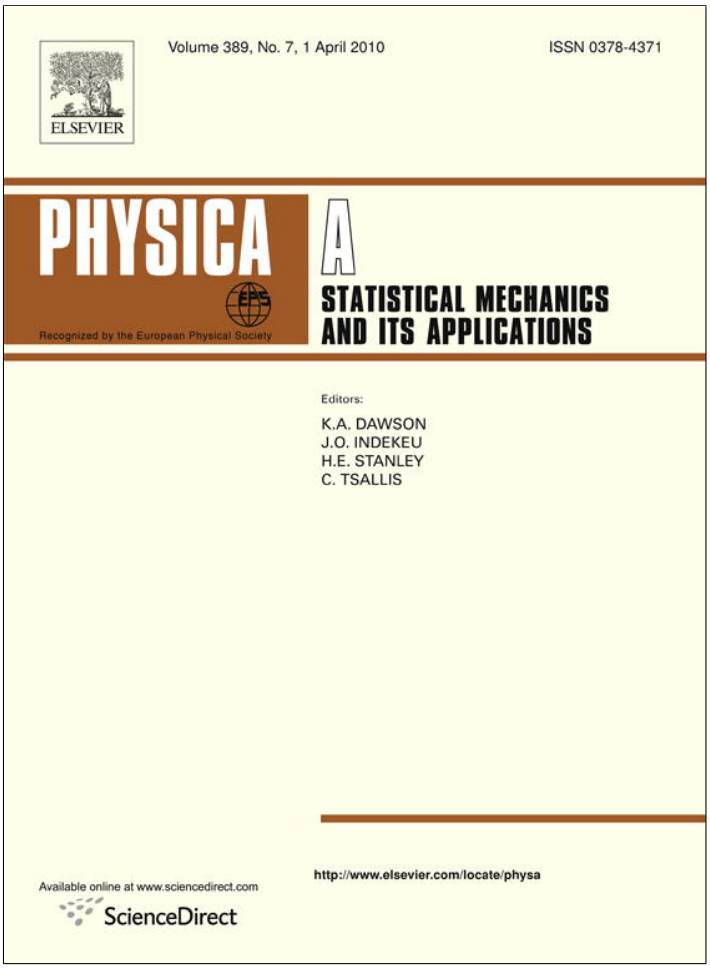

Physica A 389 (2010) 1329–1345

Contents lists available at ScienceDirect

Physica A

journal homepage: www.elsevier.com/locate/physa

Solutions to a reduced Poisson–Nernst–Planck system and determination of reaction rates

Bo Li [a,b,*], Benzhuo Lu [c], Zhongming Wang [d,a], J. Andrew McCammon [d,e,f,b]

[a] Department of Mathematics, University of California, San Diego, 9500 Gilman Drive, Mail code: 0112. La Jolla, CA 92093-0112, USA
[b] Center for Theoretical Biological Physics, University of California, San Diego, 9500 Gilman Drive, Mail code: 0374. La Jolla, CA 92093-0374, USA
[c] Institute of Computational Mathematics and Scientific/Engineering Computing, Chinese Academy of Sciences, Beijing, 100190, China
[d] Department of Chemistry and Biochemistry, University of California, San Diego, 9500 Gilman Drive, Mail code: 0365. La Jolla, CA 92093-0363, USA
[e] Department of Pharmacology, University of California, San Diego, La Jolla, CA 92093-0365, USA
[f] Howard Hughes Medical Institute, University of California, San Diego, La Jolla, CA 92093-0365, USA

ARTICLE INFO

Article history:
Received 28 May 2009
Received in revised form 14 November 2009
Available online 24 December 2009

Keywords:
Electro-diffusion
Reaction rates
Ionic concentrations
Boltzmann distributions
The Debye–Hückel approximation
The Poisson–Nernst–Planck system
Semi-analytical solution
Iteration method

ABSTRACT

We study a reduced Poisson–Nernst–Planck (PNP) system for a charged spherical solute immersed in a solvent with multiple ionic or molecular species that are electrostatically neutralized in the far field. Some of these species are assumed to be in equilibrium. The concentrations of such species are described by the Boltzmann distributions that are further linearized. Others are assumed to be reactive, meaning that their concentrations vanish when in contact with the charged solute. We present both semi-analytical solutions and numerical iterative solutions to the underlying reduced PNP system, and calculate the reaction rate for the reactive species. We give a rigorous analysis on the convergence of our simple iteration algorithm. Our numerical results show the strong dependence of the reaction rates of the reactive species on the magnitude of its far field concentration as well as on the ionic strength of all the chemical species. We also find non-monotonicity of electrostatic potential in certain parameter regimes. The results for the reactive system and those for the non-reactive system are compared to show the significant differences between the two cases. Our approach provides a means of solving a PNP system which in general does not have a closed-form solution even with a special geometrical symmetry. Our findings can also be used to test other numerical methods in large-scale computational modeling of electro-diffusion in biological systems.

1. Introduction

Concentrations of ionic and molecular species are key quantities in the description of biomolecular processes at nanometer to submicron scales. For instance, the concentrations of ligands (substrates), receptors (enzymes), and ions regulate almost all biomolecular and cellular activities. Variations in such concentrations often result from molecular diffusion, reaction, and production or depletion. As the random motion arising from thermal fluctuations, molecular diffusion causes the spread of localized signals for intracellular and intercellular communications. Chemical reaction and enzymatic regulation are also associated with the diffusion, production, and depletion of molecular species. This way, molecular diffusion and enzyme reaction form a coupled system which is often associated with signal transduction, gene expression, and metabolism networking.

* Corresponding address: Department of Mathematics, University of California at San Diego, 9500 Gilman Drive, La Jolla, CA 92093-0112, USA. Tel.: +1 858 534 6932.
E-mail addresses: bli@math.ucsd.edu (B. Li), bzlu@lsec.cc.ac.cn (B. Lu), z2wang@math.ucsd.edu (Z. Wang), jmccammon@ucsd.edu (J.A. McCammon).

0378-4371/$ – see front matter © 2009 Elsevier B.V. All rights reserved.
doi:10.1016/j.physa.2009.12.024

Biomolecular diffusion is often driven by an electric field. In such electro-diffusion, the electrostatics can strongly affect the diffusion which in turn affects the rate of association between molecules such as the binding of a ligand to a receptor; cf. e.g., Refs. [1,2]. The electric field in a charged biomolecular system is determined not only by target macromolecules but also by the concentrations of all the charged species, including diffusive ions and small charged molecules.

Mean-field approximations of diffusive molecules or ions are often given by the system of Poisson–Nernst–Planck (PNP) equations. Such a system describes properly the coupling of electrostatics and diffusion of charged chemical species. The PNP system is a combination of Nernst–Planck equations and Poisson equation. The Nernst–Planck equations describe the time evolution of concentrations of chemical species. They are of the form

$$\frac{\partial c_i}{\partial t} - \nabla \cdot [D_i(\nabla c_i + \beta q_i c_i \nabla \psi)] = 0,$$

where $c_i = c_i(x, t)$ is the local concentration of the ith charged molecular or ionic species with charge q_i at the spatial point x at time t, D_i the diffusion constant, and β the inverse thermal energy. The Poisson equation, given by

$$\nabla \cdot \varepsilon \nabla \psi = -\rho,$$

relates the electrostatic potential ψ and the charge density ρ that consists of both fixed and mobile charges, the latter being a linear combination of all the concentrations c_i. Here ε is the product of the dielectric coefficient and the vacuum permittivity ε_0. (More details of these equations are given in the next section.)

In case of no chemical reaction, the steady-state Nernst–Planck equations lead to the Boltzmann distributions of concentrations in terms of the electrostatic potential [3]. The Poisson equation then becomes the Poisson–Boltzmann equation [4–10]. For reactive chemical species, the non-equilibrium charge distributions deviate from the Boltzmann distribution, and the Poisson equation is needed to determine the electrostatic field. In this case, the PNP system can then be used to calculate the reaction rate. Such calculations are important, as recent studies have shown that substrate concentrations affect the reaction rates, a fact that is ignored in the usual Debye–Hückel limiting law [3,11].

The PNP system can be hardly solved analytically, even for the steady-state system with a very simple geometry. The main difficulty arises from the nonlinear coupling of the electrostatic potential and concentrations of chemical species. Numerical methods for PNP systems have been developed for simple one-dimensional settings and complex three-dimensional models, and have been combined with the Brownian dynamics simulations; cf. Refs. [12–21].

In this work, we consider a reduced PNP system for diffusion of ionic or molecular species in a solution in an electric field induced by charged molecules. The modification from the full PNP system is made by assuming that the concentration of each non-reactive molecular species is given by the Boltzmann distribution. Such distributions are linearized, mimicking the Debye–Hückel approximation. The concentration fields to be determined are those of reactive species. We focus on a spherical, uniformly charged solute particle in a solvent with multiple molecular or ionic species, and only consider the steady-state of the system. We first derive semi-analytical solutions of the underlying, reduced PNP system. We then present a simple iteration method for numerically solving the system using our semi-analytical solution formula. The convergence of our numerical method is proved. We further calculate numerically the equilibrium concentrations, electrostatic potential, and the reaction rates of reactive species. We finally compare our result with that of the case of no reactive species. Our work provides a means of solving a PNP system which in general does not have a closed-form solution even with a special geometrical symmetry. Our findings can also be used to test other numerical methods in large-scale computational modeling of electro-diffusion in biological systems.

In Section 2, we describe our reduced PNP system. In Section 3, we derive the semi-analytical solution formula and present our numerical scheme for obtaining the solution. In Section 4, we use our formula and scheme to calculate the electrostatic potential, the molecular or ionic concentrations, and the reaction rates of reactive species. In Section 5, we compare our results with the case that all the chemical species are non-reactive. Finally, in Section 6, we draw conclusions. In Appendix A, we give details of our derivation of our semi-analytical solution formulas; in Appendix B, we prove the convergence of our numerical scheme.

2. Model description

We first describe our reduced Poisson–Nernst–Planck (PNP) system for a general case in which some charged solutes are immersed in a solvent. There are multiple, diffusive ionic or molecular species in the solvent. Some of them are reactive and some are not. We then describe our reduced PNP system for a uniformly charged spherical solute in a solvent with multiple ionic or molecular species.

2.1. The general case

Let Ω denote the entire region of an underlying solvation system. Let Ω_m and Ω_s denote the solute region and solvent region, respectively. Let also Γ denote the interface that separates Ω_s and Ω_m, cf. Fig. 2.1. We shall use the interface Γ as the dielectric boundary. Let ε_m and ε_s denote the dielectric constant of the solute region Ω_m and that of the solvent region

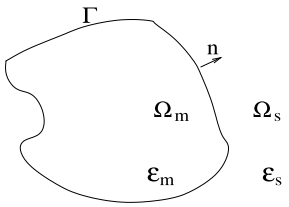

Fig. 2.1. The entire region of a solvation system Ω is divided into the solute region Ω_m and the solvent region Ω_s by the dielectric boundary Γ.

Ω_s, respectively. We define

$$\varepsilon(x) = \begin{cases} \varepsilon_m \varepsilon_0 & \text{if } x \in \Omega_m, \\ \varepsilon_s \varepsilon_0 & \text{if } x \in \Omega_s. \end{cases}$$

We assume that the solutes are charged with a fixed charge density $\rho_f = \rho_f(x)$ distributed over the solute region Ω_m. We also assume that there are M ionic or molecular species in the solvent. We denote by $c_i(x)$ the local concentration of the ith such chemical species at a spatial point x in the solvent region Ω_s. The mobile local charge density in the solvent region is given by

$$\rho_i(x) = \sum_{j=1}^{M} q_j c_j(x) \quad \text{for any } x \in \Omega_s,$$

where $q_j = z_j e$ with z_j the valence of jth species and e the elementary charge. We recall for any region D in the space that the characteristic function $\chi_D = \chi_D(x)$ is defined by $\chi_D(x) = 1$ if $x \in D$ and $\chi_D(x) = 0$ if $x \notin D$. With the characteristic functions χ_{Ω_m} and χ_{Ω_s}, the total charge density $\rho = \rho(x)$ of the entire system region is then given by

$$\begin{aligned} \rho(x) &= \chi_{\Omega_m}(x)\rho_f(x) + \chi_{\Omega_s}(x)\rho_i(x) \quad \text{if } x \in \Omega \\ &= \begin{cases} \rho_f(x) & \text{if } x \in \Omega_m, \\ \rho_i(x) & \text{if } x \in \Omega_s. \end{cases} \end{aligned}$$

The full Poisson–Nernst–Planck (PNP) system that models the diffusive ionic or molecular species consists of the following equations:

$$\frac{\partial c_i}{\partial t} = \nabla \cdot [D_i(\nabla c_i + \beta q_i c_i \nabla \psi)] \quad \text{for } x \in \Omega_s \text{ and } t > 0,\ i = 1, \ldots, M, \tag{2.1}$$

$$\nabla \cdot \varepsilon \nabla \psi = -\rho \quad \text{for } x \in \Omega \text{ and } t > 0, \tag{2.2}$$

together with some initial and boundary conditions. Here, ψ is the electrostatic potential. All the concentrations $c_1, \ldots, c_M$ and the potential ψ can depend on time t. The parameters $D_1, \ldots, D_M$ are diffusion constants. We shall only consider steady-state solutions to this PNP system. Therefore, we set the time-derivative terms to zero and assume that all the concentrations and the electrostatic potential are independent on time.

We assume that the boundary conditions for the entire system are given by

$$\begin{aligned} &c_i(\infty) = c_i^\infty, \quad i = 1, \ldots, M, \\ &\psi(\infty) = 0, \end{aligned}$$

in the case that $\Omega = \mathbb{R}^3$ is the entire space, and by

$$\begin{aligned} &c_i(x) = c_i^\infty \quad \text{for } x \in \partial\Omega,\ i = 1, \ldots, M, \\ &\psi(x) = 0 \quad \text{for } x \in \partial\Omega, \end{aligned}$$

in the case that Ω is not the entire space but rather has a nonempty boundary $\partial\Omega$, where $c_1^\infty, \ldots, c_M^\infty$ are given positive numbers that represent the bulk concentrations.

We assume that the first m species ($1 \le m < M$) are reactive and the others are non-reactive. These are defined through the boundary conditions for the concentrations on the interface Γ as follows:

$$c_i = 0 \quad \text{on } \Gamma,\ i = 1, \ldots, m, \tag{2.3}$$

$$\frac{\partial c_i}{\partial n} + \beta q_i c_i \frac{\partial \psi}{\partial n} = 0 \quad \text{on } \Gamma, i = m+1, \ldots, M, \tag{2.4}$$

where $\partial/\partial n$ denotes the normal derivative with the unit normal $\mathbf{n}$ pointing from the solute region Ω_m to the solvent region Ω_s, cf. Fig. 2.1. The condition (2.3) means that when an ion or molecule of the ith species hits the boundary Γ, it disappears due to chemical reaction. Notice that the flux of the ith species is defined by

$$\mathbf{J}_i = -D_i(\nabla c_i + \beta q_i c_i \nabla \psi).$$

Consequently, the diffusion equation and the no-flux boundary condition are given respectively by

$$\frac{\partial c_i}{\partial t} + \nabla \cdot \mathbf{J}_i = 0 \quad \text{and} \quad \mathbf{J}_i \cdot \mathbf{n} = 0,$$

which are exactly (2.1) and (2.4), respectively.

For the non-reactive species ($m < i \leq M$), the steady-state diffusion equations, the boundary conditions, and the corresponding no-flux boundary conditions on Γ in fact lead to the Boltzmann distributions $c_i(x) = c_i^\infty e^{-\beta q_i \psi(x)}$ for any $x \in \Omega_s$ and all $i = m+1, \ldots, M$. This means that $c_{m+1}, \ldots, c_M$ are all in equilibrium. Therefore, the only concentrations that are unknown variables are those of reactive species $c_1, \ldots, c_m$. Our steady-state PNP system becomes

$$\begin{aligned}
&\nabla \cdot (\nabla c_i + \beta q_i c_i \nabla \psi) = 0 \quad \text{in } \Omega_s,\ i = 1, \ldots, m,\\
&c_i = 0 \quad \text{on } \Gamma,\ i = 1, \ldots, m,\\
&c_i = c_i^\infty \quad \text{on } \partial\Omega,\ i = 1, \ldots, m,\\
&\nabla \cdot \varepsilon \nabla \psi = -\chi_{\Omega_m} \rho_f - \chi_{\Omega_s} \sum_{i=m+1}^{M} q_i c_i^\infty e^{-\beta q_i \psi} - \chi_{\Omega_s} \sum_{i=1}^{m} q_i c_i \quad \text{in } \Omega, \qquad (2.5)\\
&\psi = 0 \quad \text{on } \partial\Omega.
\end{aligned}$$

We now assume the electrostatic neutrality in the far field of the solvent: $\sum_{i=1}^{M} q_i c_i^\infty = 0$. With this assumption, we obtain the small potential approximation

$$\sum_{i=m+1}^{M} q_i c_i^\infty e^{-\beta q_i \psi} \approx \sum_{i=m+1}^{M} q_i c_i^\infty (1 - \beta q_i \psi) = -\sum_{i=1}^{m} q_i c_i^\infty - \varepsilon_s \kappa^2 \psi,$$

where

$$\kappa = \sqrt{\frac{\beta \sum_{i=m+1}^{M} q_i^2 c_i^\infty}{\varepsilon_s}}. \qquad (2.6)$$

This can be viewed as a parameter of partial ionic strength. The Poisson equation (2.5) for the electrostatic potential ψ can now be approximated by

$$\nabla \cdot \varepsilon \nabla \psi - \chi_{\Omega_s} \varepsilon_s \kappa^2 \psi = -\chi_{\Omega_m} \rho_f - \chi_{\Omega_s} \sum_{i=1}^{m} q_i \left(c_i - c_i^\infty\right) \quad \text{in } \Omega.$$

To summarize, our reduced PNP system is

$$\begin{aligned}
&\nabla \cdot (\nabla c_i + \beta q_i c_i \nabla \psi) = 0 \quad \text{in } \Omega_s,\ i = 1, \ldots, m, && (2.7)\\
&c_i = 0 \quad \text{on } \Gamma,\ i = 1, \ldots, m, && (2.8)\\
&c_i = c_i^\infty \quad \text{on } \partial\Omega,\ i = 1, \ldots, m, && (2.9)\\
&\nabla \cdot \varepsilon \nabla \psi - \chi_{\Omega_s} \varepsilon_s \kappa^2 \psi = -\chi_{\Omega_m} \rho_f - \chi_{\Omega_s} \sum_{i=1}^{m} q_i \left(c_i - c_i^\infty\right) \quad \text{in } \Omega, && (2.10)\\
&\psi = 0 \quad \text{on } \partial\Omega. && (2.11)
\end{aligned}$$

2.2. The case of a spherical solute

We assume now that the solute region Ω_m is a sphere centered at the origin with radius a, cf. Fig. 2.2, Thus, the solute region, the solvent region, and the solute–solvent interface are given respectively by

$$\Omega_m = \{x : |x| < a\}, \qquad \Omega_s = \{x \in \mathbb{R}^3 : |x| > a\}, \qquad \Gamma = \{x \in \mathbb{R}^3 : |x| = a\}.$$

We assume that the fixed charge density is a constant: $\rho_f(x) = Q$ in Ω_m. We also assume as before that only the first m species are reactive and the others are not. From (2.7)–(2.11), we have

$$\begin{aligned}
&\nabla \cdot (\nabla c_i + \beta q_i c_i \nabla \psi) = 0 \quad \text{if } |x| > a, i = 1, \ldots, m, && (2.12)\\
&c_i = 0 \quad \text{if } |x| = a,\ i = 1, \ldots, m, && (2.13)\\
&c_i(\infty) = c_i^\infty, \quad i = 1, \ldots, m, && (2.14)\\
&\nabla \cdot \varepsilon \nabla \psi - \chi_{\Omega_s} \varepsilon_s \kappa^2 \psi = -\chi_{\Omega_m} Q - \chi_{\Omega_s} \sum_{i=1}^{m} q_i \left(c_i - c_i^\infty\right) \quad \text{in } \mathbb{R}^3, && (2.15)\\
&\psi(\infty) = 0. && (2.16)
\end{aligned}$$

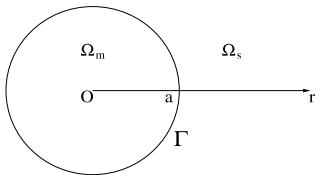

Fig. 2.2. The geometry of a spherical solute.

We observe that Eq. (2.15) for the potential ψ is equivalent to the following equations and jump conditions [9]

$$\Delta\psi = -\frac{Q}{\varepsilon_m} \quad \text{if } |x| < a, \tag{2.17}$$

$$\Delta\psi - \kappa^2\psi = -\sum_{i=1}^{m} \frac{q_i}{\varepsilon_s}\left(c_i - c_i^\infty\right) \quad \text{if } |x| > a, \tag{2.18}$$

$$[\![\psi]\!] = [\![\varepsilon\nabla\psi \cdot \mathbf{n}]\!] = 0 \quad \text{on } \Gamma, \tag{2.19}$$

where the jump $[\![u]\!]$ across Γ for any function u is defined by $[\![u]\!] = u|_{\Omega_s} - u|_{\Omega_m}$ on Γ.

3. Semi-analytical and numerical solutions

In this section, we solve semi-analytically and numerically the boundary-value problem (2.12)–(2.16).

3.1. Semi-analytical solutions

Our system (2.12)–(2.16) is radially symmetric. Hence all the concentrations $c_1, \ldots, c_M$ and the potential ψ are functions of $r = |x|$. With a series of calculations presented in Appendix A, we obtain the following semi-analytical solution

$$\psi(r) = \begin{cases} -\dfrac{Q}{6\varepsilon_m}r^2 + K_2 & \text{if } r < a, \\ \hat{C}_1\dfrac{e^{\kappa r}}{r} + \hat{C}_2\dfrac{e^{-\kappa r}}{r} - \dfrac{e^{\kappa r}}{2\kappa r}\displaystyle\int_a^r se^{-\kappa s}\hat{d}(s)ds + \frac{e^{-\kappa r}}{2\kappa r}\int_a^r se^{\kappa s}\hat{d}(s)ds & \text{if } r > a, \end{cases} \tag{3.1}$$

$$c_i(r) = c_i^\infty\left(\int_a^\infty s^{-2}e^{\beta q_i\psi(s)}ds\right)^{-1} e^{-\beta q_i\psi(r)}\int_a^r s^{-2}e^{\beta q_i\psi(s)}ds \quad \text{if } r > a,\ i = 1, \ldots, m, \tag{3.2}$$

where

$$\hat{d}(r) = \sum_{i=1}^{m}\frac{q_i}{\varepsilon_s}\left[c_i(r) - c_i^\infty\right], \tag{3.3}$$

and the integration constants are

$$\hat{C}_1 = \frac{1}{2\kappa}\int_a^\infty se^{-\kappa s}\hat{d}(s)ds, \tag{3.4}$$

$$\hat{C}_2 = \frac{Qa^3e^{\kappa a}}{3\varepsilon_s(\kappa a + 1)} + \frac{e^{2\kappa a}(\kappa a - 1)}{2\kappa(\kappa a + 1)}\int_a^\infty se^{-\kappa s}\hat{d}(s)ds, \tag{3.5}$$

$$K_2 = \frac{Qa^2}{6\varepsilon_m} + \frac{Qa^2}{3\varepsilon_s(\kappa a + 1)} + \frac{e^{\kappa a}}{\kappa a + 1}\int_a^\infty se^{-\kappa s}\hat{d}(s)ds. \tag{3.6}$$

Notice that all these integration constants depend on the function $\hat{d} = \hat{d}(r)$ which in turn depends on all the unknown functions $c_1 = c_1(r), \ldots, c_m = c_m(r)$. In (3.1), $\psi(r)$ is given as a functional of $c_1(r), \ldots, c_m(r)$ through $\hat{d}(r)$ that is defined in (3.3). In (3.2), $c_1(r), \ldots, c_m(r)$ are presented through the potential $\psi(r)$.

3.2. Numerical solutions

We use the semi-analytical solution formulas (3.1)–(3.6) to find numerical solutions of $c_1, \ldots, c_m$ and ψ. To do so, we first construct initial concentrations $(c_1^{(0)}, \ldots, c_m^{(0)})$. We then use (3.1) with c_i replaced by $c_i^{(0)} (i = 1, \ldots, m)$ to compute $\psi^{(1)}$. Next, we use (3.2) with ψ replaced by $\psi^{(1)}$ to compute $c_1^{(2)}, \ldots, c_m^{(2)}$. We repeat this process until an error tolerance is reached. In practice, we choose a finite interval to replace $[a, \infty)$.

Table 3.1
The L^∞ errors in the convergence test.

Δr	L^∞ error of c_1	Order	L^∞error of ψ	Order
1	28.3950	–	0.0070	–
1/2	20.9970	0.4355	0.0036	0.9768
1/4	11.9072	0.8183	0.0018	1.0011
1/8	6.0658	0.9731	0.0009	1.0251
1/16	2.9848	1.0231	0.0004	1.0513
1/32	1.4072	1.0848	0.0002	1.1024
1/64	0.6056	1.2164	0.0001	1.2241
1/128	0.2023	1.5820	0.0000	1.5859

Algorithm.

Step 1. Choose a number $A \gg a$ and discretize the interval $[a, A]$ with a uniform grid size Δr. Choose an error tolerance $\delta > 0$. Construct an initial guess:

$$c_i^{(0)}(r) = \frac{c_i^\infty (r-a)}{A-a} \quad \text{if } a \le r \le A,\ i = 1, \ldots, m.$$

Set $n = 0$.

Step 2. Calculate $\psi^{(n)} = \psi^{(n)}(r)$ $(a \le r \le A)$, using (3.1) (the part $r > a$) with $c_i^{(n)}$ replacing c_i $(1 \le i \le m)$ and A replacing ∞, respectively.

Step 3. Calculate $c_i^{(n+1)} = c_i^{(n+1)}(r)$ $(a \le r \le A)$ for $i = 1, \ldots, m$ using (3.2) with $c_i^{(n+1)}$ replacing c_i $(1 \le i \le m)$, $\psi^{(n)}$ replacing ψ, and A replacing ∞, respectively.

Step 4. If

$$\frac{\max\limits_{1\le i\le m} \|c_i^{(n+1)} - c_i^{(n)}\|_{L^\infty(a,A)}}{\max\limits_{1\le i\le m} \|c_i^{(n)}\|_{L^\infty(a,A)}} < \delta,$$

then stop. Otherwise set $n := n + 1$ and go to Step 2.

In all of our numerical calculations, we choose our parameters the same as or close to those in Ref. [3], mimicking some real systems. Our main parameters are:

$$M = 3, \qquad m = 1, \qquad a = 1\ \text{Å}, \qquad A = 100\ \text{Å}, \qquad \varepsilon_m = 2, \qquad \varepsilon_s = 80, \qquad \beta = 1/0.59\ \text{mol/cal}, \tag{3.7}$$

where the temperature $T = 300$ K. Our tests indicate that the value A we choose is large enough so that the underlying problem on the infinite interval (a, ∞) is well approximated by that on the finite interval (a, A). Other parameters are Q, q_1, c_1^∞, and κ. They will be specified later. As in Ref. [3], we introduce the parameter

$$I := \frac{1}{2}\sum_1^3 q_i^2 c_i^\infty.$$

Notice that the summation is taken over all the species, rather than those of non-reactive ones as in the definition of κ (cf. (2.6)). Clearly, when other parameters are given, the parameters I and κ determine each other. The units for the electrostatic potential ψ is kcal/mol e with e being the elementary charge.

We have performed a convergence test on our numerical algorithm. In this test, we choose our parameters as in (3.7) and

$$Q = 3/(4\pi)\ \text{e Å}^{-3}, \qquad q_1 = -e, \qquad q_2 = e, \qquad q_3 = -e, \qquad c_1^\infty = 50\ \text{mM}, \qquad I = 100\ \text{mM}.$$

In Table 3.1, we show the L^∞ error and order of convergence of our numerical scheme. The L^∞ error is defined to be the ratio of the discrete maximum norm of the difference of our numerical solution and that of a reference solution which is obtained using the same numerical method but with a very fine mesh. The order of convergence is defined to be $\log_2(e_{L^\infty}(\Delta r)/e_{L^\infty}(\Delta r/2))$, where $e(\Delta r)$ and $e(\Delta r/2)$ are the L^∞ error corresponding to the step size Δr and that to $\Delta r/2$, respectively. In Fig. 3.1, we show the log–log plot of the error for both the concentration c_1 and the electrostatic potential ψ. From these, we find that our numerical algorithm converges with the order of convergence close to 1 for both the concentration c_1 and the potential ψ.

We now give a convergence analysis for the general case. For convenience, let us denote $c = (c_1, \ldots, c_m)$ and write the solutions (3.1) and (3.2), in the interval (a, ∞), in the following operator forms, respectively:

$$\psi = P[c], \tag{3.8}$$

$$c = T[\psi] = (T_1[\psi], \ldots, T_m[\psi]). \tag{3.9}$$

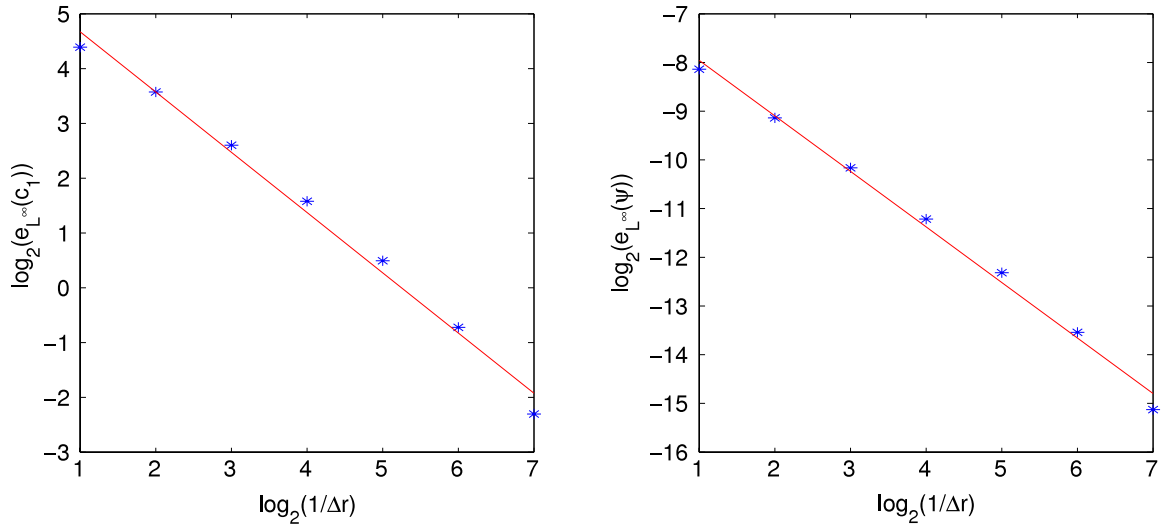

Fig. 3.1. The log–log plot of the error $e_{L^\infty}(c_1)$ and $e_{L^\infty}(\psi)$ vs. $1/\Delta r$. The slope of the solid line on left is 1.10 and that on right is 1.14.

This means that $P[c]$ is the function of $r > a$ given by (3.1) (the part for $r > a$), and $T_i[\psi]$ is the function of $r > a$ given by (3.2). With these notations, our algorithm is then as follows: Choose $c^{(0)} \in (L^\infty(a, \infty))^m$. Compute

$$\psi^{(k)} = P\left[c^{(k)}\right] \quad \text{and} \quad c^{(k+1)} = T\left[\psi^{(k)}\right], \quad k = 0, 1, \ldots. \tag{3.10}$$

The following lemma shows that P and $T_1, \ldots, T_m$ define continuous operators from respective spaces; its proof is given in Appendix B.

Lemma 3.1. (1) *If $c = (c_1, \ldots, c_m) \in (L^\infty(a, \infty))^m$ then $P[c] \in L^\infty(a, \infty)$. Moreover, $P : (L^\infty(a, \infty))^m \to L^\infty(a, \infty)$ is continuous.*

(2) *If $\psi \in L^\infty(a, \infty)$ then $T_i[\psi] \in L^\infty(a, \infty)$ for all $i = 1, \ldots, m$. Moreover, $T[\psi] = (T_1[\psi], \ldots, T_m[\psi])$ defines a continuous mapping $T : L^\infty(a, \infty) \to (L^\infty(a, \infty))^m$.*

To state and prove our main convergence result, we need the following:

Lemma 3.2. *Let $\hat{a} > 0$ and $\hat{b} > 0$ be such that $\hat{a}\hat{b} < \mathrm{e}^{-1}$. Let $f(x) = \hat{a}\mathrm{e}^{\hat{b}x}$ for $x \in \mathbb{R}$.*

(1) *There exist exactly two distinct fixed points of f in $\mathbb{R}$, both being positive.*

(2) *Let $x^* = x^*(\hat{a}, \hat{b})$ be the smaller fixed point of f. Then $f(x) \le x^*$ for any $x \in [0, x^*]$.*

Proof. (1) Let $g(x) = f(x) - x$ ($x \in \mathbb{R}$). Then $g'(x) = \hat{a}\hat{b}\mathrm{e}^{\hat{b}x} - 1$ and $g''(x) = \hat{a}\hat{b}^2\mathrm{e}^{bx}$. Clearly, $g'(x)$ has a unique zero $x_m = -(1/\hat{b})\ln(\hat{a}\hat{b}) > 0$, and $g(x)$ attains its minimum at x_m with the minimum value $g(x_m) = (1 + \ln(\hat{a}\hat{b}))/\hat{b} < 0$, since $\hat{a}\hat{b} < \mathrm{e}^{-1}$. Note that $g(0) = \hat{a} > 0$ and $g(x) \to +\infty$ as $x \to +\infty$. Thus the continuous function $g(x)$ has at least one zero in $(0, x_m)$ and another zero in $(x_m, +\infty)$. These are in fact the only zeros, since $g''(x) > 0$ for all $x \in \mathbb{R}$. These two zeros of $g(x)$ are the two fixed points of $f(x)$, both positive.

(2) If $0 \le x \le x^*$ then $f(x) = \hat{a}\mathrm{e}^{\hat{b}x} \le \hat{a}\mathrm{e}^{\hat{b}x^*} = f(x^*) = x^*$. □

We define

$$\hat{a} = \left(\max_{1\le i\le m} c_i^\infty\right) \mathrm{e}^{\beta\left(\max\limits_{1\le i\le m}|q_i|\right)\left[\frac{|Q|a^2}{3\varepsilon_s(\kappa a+1)} + \frac{|\kappa a-1|+2(\kappa a+1)}{2\kappa^3 a^2}\sum\limits_{j=1}^{m}|q_j|c_j^\infty\right]}, \tag{3.11}$$

$$\hat{b} = \beta\left(\max_{1\le i\le m} c_i^\infty\right)\left(\max_{1\le i\le m}|q_i|\right)\left(\sum_{i=1}^{m}|q_i|\right)\frac{|\kappa a - 1| + 2(\kappa a + 1)}{2\kappa^3 a^2}, \tag{3.12}$$

$$\hat{A} = \frac{3\hat{a}\hat{b}}{\kappa^2\varepsilon_s \max\limits_{1\le i\le m} c_i^\infty}, \tag{3.13}$$

$$\hat{B} = \frac{\hat{b}}{\max\limits_{1\le i\le m} c_i^\infty}. \tag{3.14}$$

Let $x^* = x^*(\hat{a}, \hat{b}) > 0$ be the smaller fixed point of $f(x) = \hat{a}\mathrm{e}^{\hat{b}x}$ as defined in Lemma 3.2.

Proposition 3.1. *Assume that* $\hat{A}e^{\hat{B}x^*(\hat{a},\hat{b})} < 1$. *Assume also that* $c^{(0)} \in (L^\infty(a,\infty))^m$ *satisfies* $\|c^{(0)}\|_\infty \le x^*$. *Then the sequences* $\{\psi^{(k)}\}_{i=0}^\infty$ *and* $\{c^{(k)}\}_{i=0}^\infty$ *defined in* (3.10) *converge in* $L^\infty(a,\infty)$ *and* $(L^\infty(a,\infty))^m$ *to the solution of* (3.1) *and* (3.2), *respectively.*

The proof of this main convergence result is given in Appendix B. Here we make some remarks.

(1) In our numerical calculations that are reported in the next section, we use parameters that are compatible with those used in Ref. [3]. For such parameters, the condition of convergence is much simplified.

(2) Our convergence condition is only sufficient. Our extensive numerical tests suggest that our iteration algorithm converges if $\sum_{i=1}^m q_i^2 c_i^\infty < \sum_{i=m+1}^M q_i^2 c_i^\infty$.

(3) If our condition of convergence is not satisfied, then our algorithm may not converge. For instance, using the parameters (3.7) and

$$Q = 1/\pi \text{ e Å}^{-3}, \qquad q_1 = 2e, \qquad q_2 = q_3 = -e, \qquad c_1^\infty = c_2^\infty = c_3^\infty = 100 \text{ mM},$$

we find that the sequence $\{c_1^{(n)}\}$ produced by our algorithm does not converge.

4. Numerical results of concentrations, potential, and reaction rates

We now report our results of numerical calculations. We use the parameters in (3.7) and

$$c_1^\infty = 50 \text{ mM}, \qquad q_1 = -e, \qquad q_2 = e, \qquad q_3 = -e, \qquad I = 100 \text{ mM}. \tag{4.1}$$

Several different values of the constant charge density Q are chosen for our calculations.

4.1. Concentrations and potential

Fig. 4.1 shows our numerical solution of the electrostatic potential $\psi(r)$ and the concentration $c_1(r)$ with $Q = 3/(4\pi)$ e Å^{-3} and $Q = -3/(4\pi)$ e Å^{-3}, respectively. The change of the sign of Q does not affect the concentration $c_1(r)$ but changes the sign of the electrostatic potential $\psi(r)$. Notice that the potential is monotonic in these cases.

We now keep the same set of parameters except changing Q so that its magnitude is very small. Fig. 4.2 shows the numerical solution of the potential $\psi(r)$ and concentration $c_1(r)$ with $Q = 0.0025$ e Å^{-3} and $Q = -0.0025$ e Å^{-3}, respectively. We see clearly that the potential is no longer monotonic.

The non-monotonicity of potential can be seen from our semi-analytic solution formula (3.1) for the case of $M = 3$ (three ionic or molecular species) and $m = 1$ (one reactive species). If Q and q_1 have the same sign, then there exists a range of Q values such that the potential is non-monotonic. In fact, let us assume for example that $q_1 < 0$ and $Q < 0$. By (3.1) and (3.6) we have

$$\psi(a) = \frac{Qa^2}{3\varepsilon_s(\kappa a + 1)} + \frac{e^{\kappa a}}{\kappa a + 1}\int_a^\infty s e^{-\kappa s}\hat{d}(s)\mathrm{d}s. \tag{4.2}$$

Here for the case $m = 1$ we have $\hat{d}(r) = (q_1/\varepsilon_s)[c_i(r) - c_1^\infty]$. In general, we have $c_1(r) \le c_1^\infty$ for all $r \ge a$. If this is so, then we have from (4.2) that $\psi(a) > 0$ if $Q > 0$ is small enough. On the other hand, we have from (3.1) and the continuity condition (2.19) that $\psi'(a+) > 0$. This means that the potential increases near $a+$. But $\psi(+\infty) = 0$ by (2.16). Therefore, the potential is not monotonic.

4.2. Reaction rates

We define the reaction rate for the ith ($1 \le i \le m$) reactive species to be $R_i = c_i'(a)/c_i^\infty$. By (3.2) and a straightforward calculation, we have $R_i = \left(a^2\int_a^\infty s^{-2}e^{\beta q_i\psi(s)}\mathrm{d}s\right)^{-1}$.

We fix again the parameters as in (3.7) and (4.1), and set $Q = 3/(4\pi)$ e Å^{-3}. We plot in Fig. 4.3 the reaction rate vs. ionic strength $I = (1/2)\sum_{i=1}^3 q_i^2 c_i^\infty$ for different values of the bulk concentration c_1^∞. We also plot the reaction rate R_1 vs. the bulk concentration c_1^∞ in Fig. 4.4 at different levels of ionic strength. It is clear from these plots that the reaction rate decreases as the ionic strength increases for each fixed bulk concentration c_1^∞. The rate also increases with c_1^∞ increases for each fixed I.

5. Comparison with the case of no reaction

We now consider the case that all the chemical species are non-reactive, and compare the related results with those presented in the previous section on reactive species. Non-reactive diffusive species are characterized by the non-reactive boundary condition. In this case, the concentration of each of the species satisfies the Boltzmann distribution. Therefore, the system reduces to partial differential equation for the electrostatic potential only, together with some side conditions. To

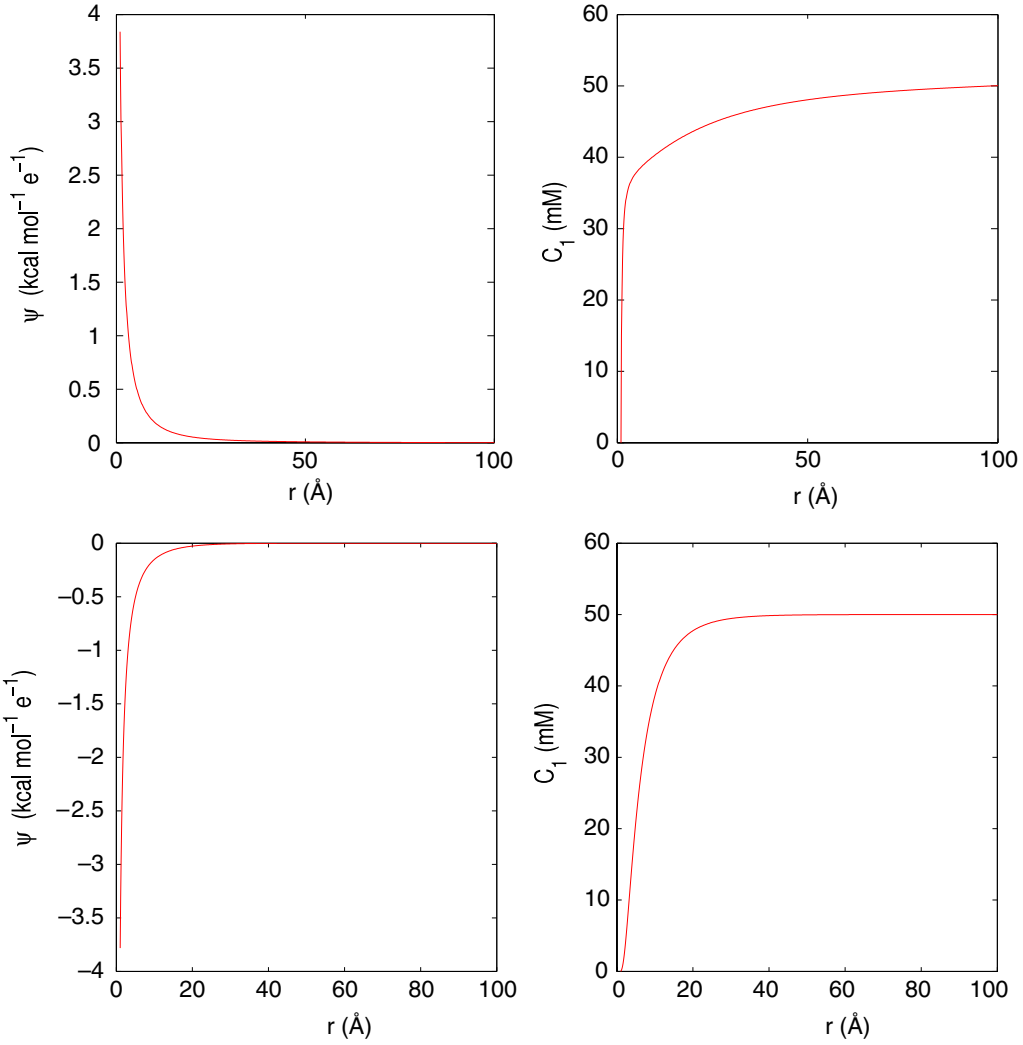

Fig. 4.1. Numerical solution of the electrostatic potential and the concentration $c_1(r)$. Top: $Q = 3/(4\pi)$ e Å^{-3}. Bottom: $Q = -3/(4\pi)$ e Å^{-3}.

make our comparison more reasonable, we linearize the concentrations $c_i(r) = c_i^\infty e^{-\beta q_i \psi}$ for $i = m+1, \ldots, M$, as before. The resulting equation and side conditions are

$$\Delta\psi = -\frac{Q}{\varepsilon_m} \quad \text{if } |x| < a, \tag{5.1}$$

$$\Delta\psi - \kappa^2\psi = -\sum_{i=1}^{m} \frac{q_i c_i^\infty}{\varepsilon_s}\left(e^{-\beta q_i \psi} - 1\right) \quad \text{if } |x| > a, \tag{5.2}$$

$$[\![\psi]\!] = [\![\varepsilon \nabla\psi \cdot \mathbf{n}]\!] = 0 \quad \text{on } \Gamma, \tag{5.3}$$

where κ is defined in (2.6). These should be compared with (2.17)–(2.19).

As before, we obtain exactly the same formula (3.1) with constants $\hat{C}_1$, $\hat{C}_2$, K_2 given by (3.4)–(3.6) but the quantity $\hat{d}(r)$ should be replaced by

$$\hat{d}(r) = \sum_{i=1}^{m} q_i c_i^\infty \left(e^{-\beta q_i \psi} - 1\right).$$

This and (3.1) can be used to numerically compute the potential.

We test the example in Section 4 with the parameters given in (3.7) and (4.1). Fig. 5.1 shows our numerical results for $Q = -3/(4\pi)$ e Å^{-3}. We find that for both of the reactive and non-reactive systems the potential $\psi(r)$ is similar and also the concentration $c_1(r)$ is similar. Here for the non-reactive case the concentration $c_1(r)$ is defined by the Boltzmann distribution.

If we change Q from $-3/(4\pi)$ e Å^{-3} to $3/(4\pi)$ e Å^{-3}, then the potential also changes sign, as seen in Figure Fig. 5.2. It is clear that the potential for the reactive case is different from that for the non-reactive case. Moreover, the concentration $c_1(r)$

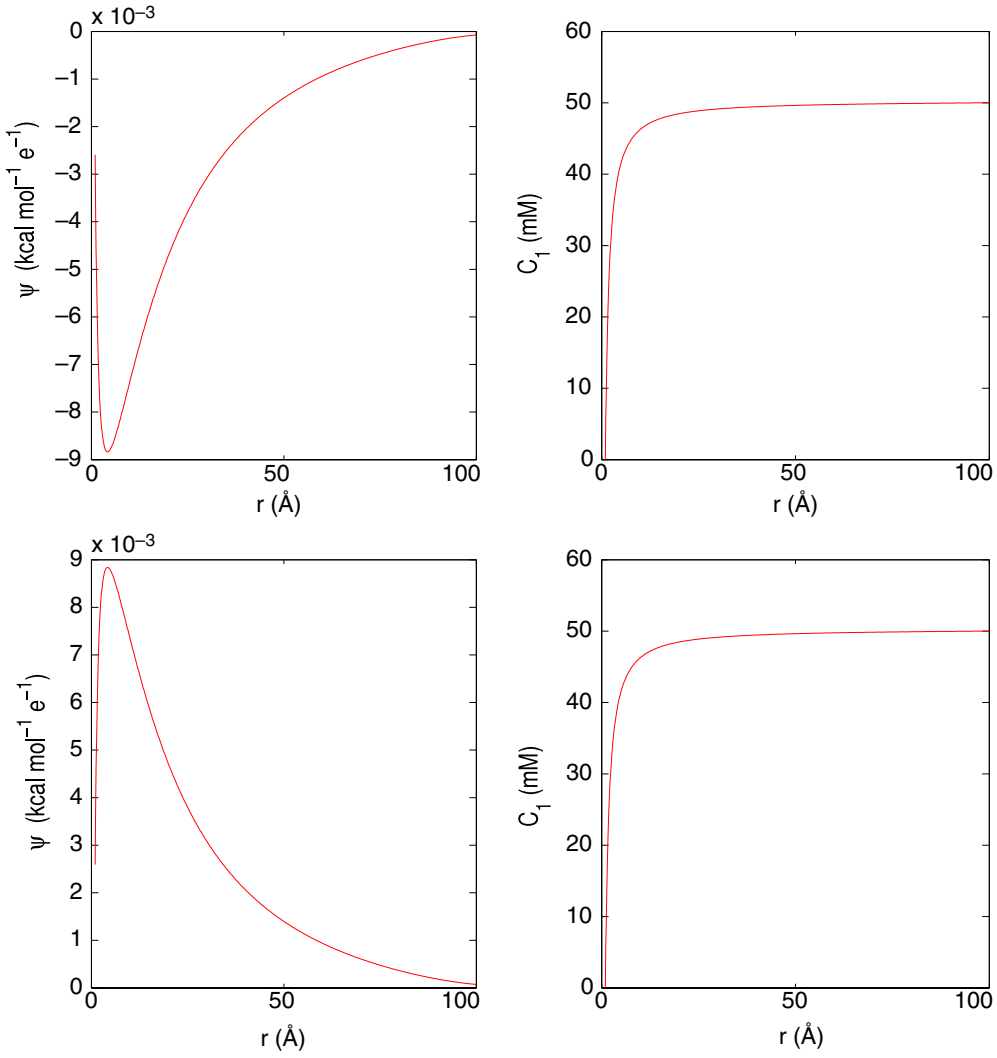

Fig. 4.2. Numerical solution of the electrostatic potential and the concentration $c_1(r)$. The potential is non-monotone. Top: $Q = 0.0025$ e Å^{-3}. Bottom: $Q = -0.0025$ e Å^{-3}.

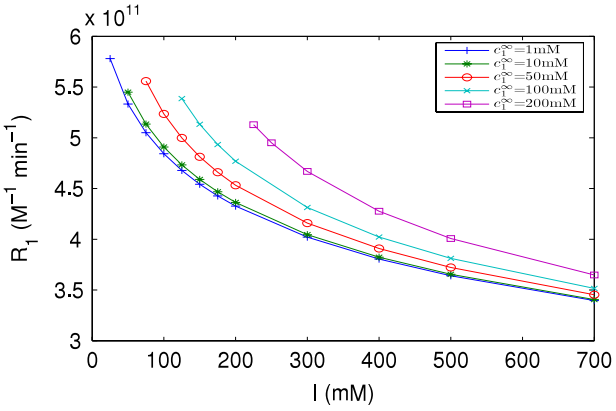

Fig. 4.3. Reaction rates R_1 vs. the ionic strength I for different bulk concentrations c_1^∞.

is quite different for these two cases. For the non-reactive case the concentration is very large near the dielectric boundary $r = a$.

Finally in Fig. 5.3 we plot our results for $Q = 0.0025$ e Å^{-3}. We see the non-monotonic behavior of the potential for the reactive system, as predicted before, but the monotonic behavior of the non-reactive system.

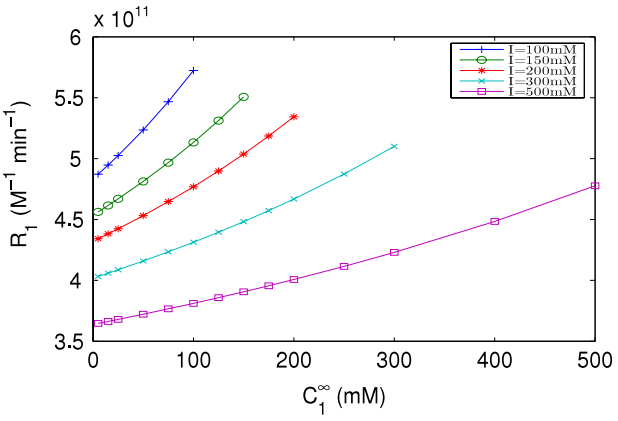

Fig. 4.4. Reaction rates R_1 vs. bulk concentration c_1^{∞} for different values of ionic strength.

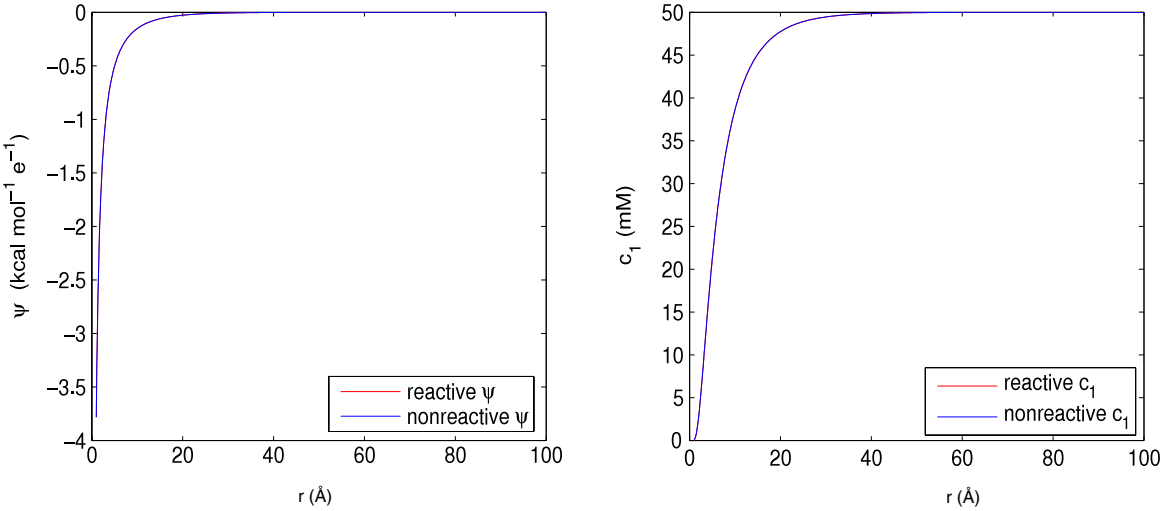

Fig. 5.1. Comparison of the reactive and non-reactive systems with $Q = -3/(4\pi)$ e Å^{-3}.

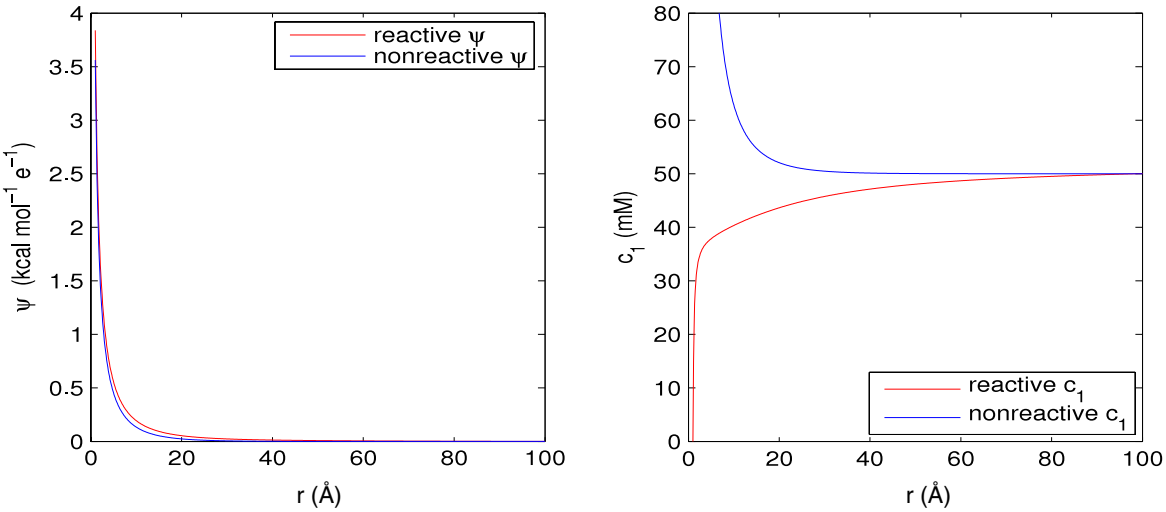

Fig. 5.2. Comparison of the reactive and non-reactive systems with $Q = 3/(4\pi)$ e Å^{-3}.

6. Conclusions and discussions

We have studied a reduced PNP system for a spherical, uniformly charged solute immersed in a solvent. We have obtained a semi-analytical solution formula which is in the form of a system of integral equations. Our simple iteration scheme based on this formulation is shown to be convergent.

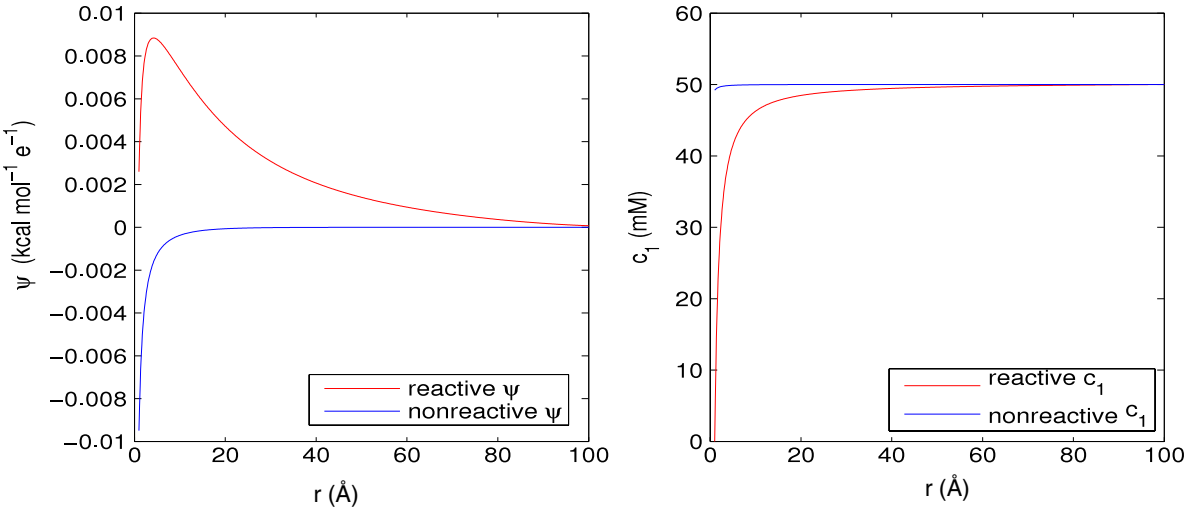

Fig. 5.3. Comparison of the reactive and non-reactive systems with $Q = 0.0025$ e Å^{-3}.

The widely used PNP system, even in its reduced form, is hard to solve analytically or numerically. Our work, though focused on the spherical geometry, has provided some solution method to such a system. Our analytical and numerical results can be used to test other methods for large-scale calculations. Our convergence analysis can also be possibly generalized to systems with a more complicated geometry.

We have numerically calculated equilibrium concentrations, electrostatic potential, and the reaction rate. Our numerical results agree with those reported in Ref. [3]. Moreover, we have discovered a new property: when the charge Q is very small in magnitude, the potential ψ can be non-monotonic. We have offered some explanation for this using our semi-analytical solution formula. We also confirmed numerically that such non-monotonicity does not exist in the case for non-reactive chemical species.

We emphasize that our detailed studies on a special case can be used to investigate other physical properties of charged solvation systems. These include the effect of substrate concentrations to reaction that is ignored in the usual Debye–Hückel limiting law [3,11], the effect of solvent excluded volume in a charged solvation system [8], and ionic distributions around charged solutes that has been studied by transformed Poisson–Boltzmann relations [22]. Our approach can be also used to study the dynamical PNP system [3].

Acknowledgements

B. Li was supported by the US National Science Foundation (NSF) through the grant DMS-0811259, by the NSF Center for Theoretical Biological Physics (CTBP) with the NSF grant PHY-0822283, and by the US Department of Energy through the grant DE-FG02-05ER25707. B. Lu was partially supported by the 100 Talents Program of the Chinese Academy of Sciences. Z. Wang and J.A. McCammaon were supported by NSF, NIH, HHMI, CTBP, NBCR, and Accelrys.

Appendix A

We present in this appendix details of the derivation of the semi-analytical solution formulas (3.1)–(3.6) to the system (2.12)–(2.16). We recall the following formulas for a smooth, radially symmetric function $u = u(r)$ with $r = |x| > 0$ and $x \in \mathbb{R}^3$:

$$\Delta u(r) = \frac{1}{r^2}\frac{\mathrm{d}}{\mathrm{d}r}\left(r^2\frac{\mathrm{d}u(r)}{\mathrm{d}r}\right); \tag{A.1}$$

$$\nabla u(r) = \frac{\mathrm{d}u(r)}{\mathrm{d}r}\frac{\vec{r}}{r}; \tag{A.2}$$

$$\nabla\cdot\left(u(r)\frac{\vec{r}}{r}\right) = \frac{\mathrm{d}u(r)}{\mathrm{d}r} + \frac{2u(r)}{r}, \tag{A.3}$$

where $\vec{r}$ denotes the position vector at a point $x \in \mathbb{R}^3$ with $|x| = r$.

Using (A.1), we obtain from (2.17) that

$$\frac{1}{r^2}\frac{\mathrm{d}}{\mathrm{d}r}\left(r^2\frac{\mathrm{d}\psi(r)}{\mathrm{d}r}\right) = -\frac{Q}{\varepsilon_m} \quad \text{if } r < a.$$

This leads to

$$\psi = -\frac{Q}{6\varepsilon_m} r^2 - K_1 r^{-2} + K_2 \quad \text{if } r < a,$$

where K_1 and K_2 are two constants. Since the spherical solute has a uniform (constant) charge density, the potential ψ should be continuous inside the spherical solute region. Thus $\psi(0) < \infty$ and hence $K_1 = 0$. Therefore,

$$\psi(r) = -\frac{Q}{6\varepsilon_m} r^2 + K_2 \quad \text{if } r < a. \tag{A.4}$$

By our notation $\hat{d}(r)$ (cf. (3.3)) and (A.1), Eq. (2.18) becomes

$$\frac{1}{r^2}\frac{\mathrm{d}}{\mathrm{d}r}\left(r^2 \frac{\mathrm{d}\psi(r)}{\mathrm{d}r}\right) - \kappa^2 \psi(r) = -\hat{d}(r), \quad r > a. \tag{A.5}$$

It is easy to verify that the corresponding homogeneous equation (i.e., the equation with $-\hat{d}(r)$ replaced by 0) has two linearly independent solutions $\mathrm{e}^{\kappa r}/r$ and $\mathrm{e}^{-\kappa r}/r$. Therefore, using the method of variation of parameters, we obtain a particular solution to the inhomogeneous equation (A.5)

$$\psi_s(r) = -\frac{\mathrm{e}^{\kappa r}}{2\kappa r}\int_a^r s\mathrm{e}^{-\kappa s}\hat{d}(s)\mathrm{d}s + \frac{\mathrm{e}^{-\kappa r}}{2\kappa r}\int_a^r s\mathrm{e}^{\kappa s}\hat{d}(s)\mathrm{d}s, \quad r > a.$$

Hence the general solution to (A.5) is

$$\psi(r) = \hat{C}_1\frac{\mathrm{e}^{\kappa r}}{r} + \hat{C}_2\frac{\mathrm{e}^{-\kappa r}}{r} - \frac{\mathrm{e}^{\kappa r}}{2\kappa r}\int_a^r s\mathrm{e}^{-\kappa s}\hat{d}(s)\mathrm{d}s + \frac{\mathrm{e}^{-\kappa r}}{2\kappa r}\int_a^r s\mathrm{e}^{\kappa s}\hat{d}(s)\mathrm{d}s, \quad r > a, \tag{A.6}$$

where $\hat{C}_1$ and $\hat{C}_2$ are two integration constants. Notice that (3.1) is just the combination of (A.4) and (A.6).

By the boundary conditions (2.13) and (2.14), each concentration field $c_i = c_i(r)$ $(1 \le i \le m)$ is bounded on $[a, \infty)$. Thus the function $\hat{d} = \hat{d}(r)$ is also continuous and bounded on $[a, \infty)$. Using (B.1), we find that the last term in (A.6) is bounded. Therefore, from the boundary condition $\psi(\infty) = 0$ (cf. (2.16)) and the first and third terms in (A.6), we must have

$$\lim_{r\to\infty}\left(\hat{C}_1 - \frac{1}{2\kappa}\int_a^r s\mathrm{e}^{-\kappa s}\hat{d}(s)\mathrm{d}s\right) = 0.$$

This implies (3.4). By the solution formulas (A.4) and (A.6), and the jump conditions (2.19) and (A.2), we have

$$-\frac{Q}{6\varepsilon_m}a^2 + K_2 = \hat{C}_1\frac{\mathrm{e}^{\kappa a}}{a} + \hat{C}_2\frac{\mathrm{e}^{-\kappa a}}{a},$$
$$-\frac{Qa}{3} = \varepsilon_s\hat{C}_1\frac{\mathrm{e}^{\kappa a}}{a}(\kappa a - 1) - \varepsilon_s\hat{C}_2\frac{\mathrm{e}^{-\kappa a}}{a}(\kappa a + 1).$$

Solving these two equations for $\hat{C}_2$ and K_2, we obtain (3.5) and (3.6).

Now we solve the boundary-value problem of diffusion equation (2.12)–(2.14). Fix i with $1 \le i \le m$. By (A.2), Eq. (2.12) becomes

$$\nabla\cdot\left[\left(\frac{\mathrm{d}c_i(r)}{\mathrm{d}r} + \beta q_i c_i(r)\frac{\mathrm{d}\psi(r)}{\mathrm{d}r}\right)\frac{\vec{r}}{r}\right] = 0. \tag{A.7}$$

Denoting

$$h_i(r) = \frac{\mathrm{d}c_i(r)}{\mathrm{d}r} + \beta q_i c_i(r)\frac{\mathrm{d}\psi(r)}{\mathrm{d}r}, \tag{A.8}$$

we have by (A.7) and (A.3) that $h_i'(r) + 2h_i(r)/r = 0$. Solving this linear first-order ordinary differential equation, we obtain $h_i(r) = K_3 r^{-2}$, with K_3 a constant. Therefore, this and (A.8) lead to

$$\frac{\mathrm{d}c_i(r)}{\mathrm{d}r} + \beta q_i\frac{\mathrm{d}\psi(r)}{\mathrm{d}r}c_i = K_3 r^{-2}.$$

This is also a linear first-order ordinary differential equation for $c_i = c_i(r)$, and can be solved. The result is

$$c_i(r) = \left(K_3\int_a^r s^{-2}\mathrm{e}^{\beta q_i\psi(s)}\mathrm{d}s + K_4\right)\mathrm{e}^{-\beta q_i\psi(r)}. \tag{A.9}$$

The boundary condition $c_i(a) = 0$ implies $K_4 = 0$. The boundary condition $c_i(\infty) = c_i^\infty$ leads to $K_3 = c_i^\infty\left(\int_a^\infty r^{-2}\mathrm{e}^{\beta q_i\psi(r)}\mathrm{d}r\right)^{-1}$. This and (A.9) lead to (3.2).

Appendix B

In this appendix, we prove Lemma 3.1 and Proposition 3.1. For convenience, we shall denote by $\|\cdot\|_\infty$ the norm of $L^\infty(a,\infty)$ or $(L^\infty(a,\infty))^m$. We recall for any nonzero $\sigma\in\mathbb{R}$ that

$$\int se^{\sigma s}ds = \frac{\sigma s-1}{\sigma^2}e^{\sigma s}. \tag{B.1}$$

Proof of Lemma 3.1. (1) Let $c_1,\dots,c_m\in L^\infty(a,\infty)$. By our definition (3.8),

$$P[c_1,\dots,c_m](r)=\hat{C}_1\frac{e^{\kappa r}}{r}+\hat{C}_2\frac{e^{-\kappa r}}{r}-\frac{e^{\kappa r}}{2\kappa r}\int_a^r se^{-\kappa s}\hat{d}(s)ds+\frac{e^{-\kappa r}}{2\kappa r}\int_a^r se^{\kappa s}\hat{d}(s)ds,\quad r>a. \tag{B.2}$$

By (3.3), we have $\hat{d}\in L^\infty(a,\infty)$. It follows from (3.5) and (B.1), together with simple calculations, that

$$\left|\hat{C}_2\frac{e^{-\kappa r}}{r}\right|\le\frac{|Q|a^2e^{\kappa a}}{3\varepsilon_s(\kappa a+1)}+\frac{|\kappa a-1|e^{\kappa a}}{2\kappa a^3}\|\hat{d}\|_\infty\quad\forall r>a.$$

For the last term in (B.2) we have

$$\left|\frac{e^{-\kappa r}}{2\kappa r}\int_a^r se^{\kappa s}\hat{d}(s)ds\right|\le\|\hat{d}\|_\infty\frac{e^{-\kappa r}}{2\kappa}\int_a^r e^{\kappa s}ds=\frac{\|\hat{d}\|_\infty}{2\kappa^2}\left[1-e^{\kappa(a-r)}\right]\le\frac{\|\hat{d}\|_\infty}{2\kappa^2}\quad\forall r>a.$$

Now consider the sum of the first and third terms in (B.2). By (3.4) and (B.1), we have

$$\left|\hat{C}_1\frac{e^{\kappa r}}{r}-\frac{e^{\kappa r}}{2\kappa r}\int_a^r se^{-\kappa s}\hat{d}(s)ds\right|=\left|\frac{e^{\kappa r}}{2\kappa r}\int_r^\infty se^{-\kappa s}\hat{d}(s)ds\right|\le\frac{\|\hat{d}\|_\infty}{2\kappa^3}\left(\frac{1}{a}+\kappa\right)\quad\forall r>a.$$

Therefore, $P[c_1,\dots,c_m]\in L^\infty(a,\infty)$.

To prove the continuity of $P:(L^\infty(a,\infty))^m\to L^\infty(a,\infty)$, we observe that P is in fact an affine operator. Therefore, similar calculations lead to

$$\|P[c]-P[\hat{c}]\|_\infty\le\mu\|c-\hat{c}\|_\infty\quad\forall c,\hat{c}\in(L^\infty(a,\infty))^m,$$

where $\mu>0$ is a constant independent of c and $\hat{c}$. Hence P is continuous.

(2) Let $\psi\in L^\infty(a,\infty)$. Fix an index i with $1\le i\le m$. We have by our definition (3.9) and (3.2) that

$$T_i[\psi](r)=c_i^\infty\left(\int_a^\infty s^{-2}e^{\beta q_i\psi(s)}ds\right)^{-1}e^{-\beta q_i\psi(r)}\int_a^r s^{-2}e^{\beta q_i\psi(s)}ds\quad\forall r>a.$$

Clearly,

$$|T_i[\psi](r)|=T_i[\psi](r)\le c_i^\infty e^{\beta|q_i|\|\psi\|_\infty}\quad\forall r>a.$$

Therefore $T_i[\psi]\in L^\infty(a,\infty)$.

To prove the continuity of $T_i:L^\infty(a,\infty)\to L^\infty(a,\infty)$, we need only to prove that each part of T_i is continuous. Let $\phi,\psi\in L^\infty(a,\infty)$. It follows from the mean-value theorem that

$$\left|e^{-\beta q_i\phi(r)}-e^{-\beta q_i\psi(r)}\right|\le\beta|q_i|e^{\beta|q_i|\max\{\|\phi\|_\infty,\|\psi\|_\infty\}}\|\phi-\psi\|_\infty\quad\forall r>a.$$

Similarly,

$$\begin{aligned}\left|\int_a^r s^{-2}e^{\beta q_i\phi(r)}dr-\int_a^r s^{-2}e^{\beta q_i\phi(r)}dr\right|&\le\beta|q_i|e^{\beta|q_i|\max\{\|\phi\|_\infty,\|\psi\|_\infty\}}\|\phi-\psi\|_\infty\int_a^r s^{-2}ds\\&\le\frac{\beta|q_i|}{a}e^{\beta|q_i|\max\{\|\phi\|_\infty,\|\psi\|_\infty\}}\|\phi-\psi\|_\infty\quad\forall r>a.\end{aligned}$$

The upper limit r can be replaced by ∞ in these integrals. All these together imply that

$$|T_i[\phi]-T_i[\psi]|\le\mu'\|\phi-\psi\|_\infty,$$

where $\mu'>0$ is a constant independent of ϕ and ψ. Therefore, each $T_i:L^\infty(a,\infty)\to L^\infty(a,\infty)$ is continuous. □

To prove Proposition 3.1, we first prove a lemma. Recall that $\hat{a}$ and $\hat{b}$ are given in (3.11) and (3.12), respectively. Recall also that $x^*=x^*(\hat{a},\hat{b})>0$ is the smaller fixed point of $f(x)=\hat{a}e^{\hat{b}x}$ as defined in Lemma 3.2. For any $c^{(0)}\in(L^\infty(a,\infty))^m$, we define by (3.10) that

$$c^{(k+1)}=T\left[P\left[c^{(k)}\right]\right]=(T\circ P)\left[c^{(k)}\right],\quad k=0,1,\dots. \tag{B.3}$$

Lemma B.1. *If $\|c^{(0)}\|_\infty\le x^*$ then $\|c^{(k)}\|_\infty\le x^*$ for all $k=1,2,\dots$.*

Proof. By induction, it suffices to show that, for any $c \in (L^\infty(a,\infty))^m$, $\|(T\circ P)[c]\|_\infty \le x^*$ if $\|c\|_\infty \le x^*$. Let $\psi = P[c]$. The definition of $P : (L^\infty(a,\infty))^m \to L^\infty(a,\infty)$ (cf. (3.8)) and the solution formula (3.1) imply that

$$\begin{aligned}\psi(r) &= P[c](r)\\ &= \left(\hat{C}_1\frac{e^{\kappa r}}{r} - \frac{e^{\kappa r}}{2\kappa r}\int_a^r se^{-\kappa s}\hat{d}(s)ds\right) + \hat{C}_2\frac{e^{-\kappa r}}{r} + \frac{e^{-\kappa r}}{2\kappa r}\int_a^r se^{\kappa s}\hat{d}(s)ds\\ &= \frac{e^{\kappa r}}{2\kappa r}\int_r^\infty se^{-\kappa s}\hat{d}(s)ds + \left(\frac{Qa^3e^{\kappa a}}{3\varepsilon_s(\kappa a+1)} + \frac{e^{2\kappa a}(\kappa a-1)}{2\kappa(\kappa a+1)}\int_a^\infty se^{-\kappa s}\hat{d}(s)ds\right)\frac{e^{-\kappa r}}{r}\\ &\quad + \frac{e^{-\kappa r}}{2\kappa r}\int_a^r se^{\kappa s}\hat{d}(s)ds \quad \forall r > a,\end{aligned}$$

where $\hat{d}(r)$ is defined in (3.3). By (B.1) we have

$$\left|\frac{e^{\kappa r}}{2\kappa r}\int_r^\infty se^{-\kappa s}\hat{d}(s)ds\right| \le \frac{e^{\kappa r}}{2\kappa r}\|\hat{d}\|_\infty\int_r^\infty se^{-\kappa s}ds = \left(\frac{1}{2\kappa^2}+\frac{1}{2\kappa^3 r}\right)\|\hat{d}\|_\infty \le \frac{1+\kappa a}{2\kappa^3 a}\|\hat{d}\|_\infty.$$

Similarly, we have

$$\left|\left(\frac{Qa^3e^{\kappa a}}{3\varepsilon_s(\kappa a+1)} + \frac{e^{2\kappa a}(\kappa a-1)}{2\kappa(\kappa a+1)}\int_a^\infty se^{-\kappa s}\hat{d}(s)ds\right)\frac{e^{-\kappa r}}{r}\right| \le \frac{|Q|a^2}{3\varepsilon_s(\kappa a+1)} + \frac{|\kappa a-1|}{2\kappa^3 a}\|\hat{d}\|_\infty,$$

and

$$\left|\frac{e^{-\kappa r}}{2\kappa r}\int_a^r se^{\kappa s}\hat{d}(s)ds\right| \le \left(\frac{\kappa r-1}{2\kappa^3 r} - \frac{\kappa a-1}{2\kappa^3 r}e^{\kappa(a-r)}\right)\|\hat{d}\|_\infty \le \frac{\kappa a+1}{2\kappa^3 a}\|\hat{d}\|_\infty.$$

Combining all these and using (3.3), we obtain

$$|\psi(r)| \le \frac{|Q|a^2}{3\varepsilon_s(\kappa a+1)} + \frac{|\kappa a-1|+2(\kappa a+1)}{2\kappa^3 a^2}\sum_{i=1}^m |q_i|(\|c_i\|_\infty + c_i^\infty). \tag{B.4}$$

Now the solution formula (3.2) and the definition of $T : L^\infty(a,\infty) \to (L^\infty(a,\infty))^m$ (3.9) imply that

$$|T_i[\psi](r)| = T_i[\psi](r) \le c_i^\infty e^{\beta|q_i|\|\psi\|_\infty} \quad \forall r > a,\ i = 1,\dots,m.$$

This and (B.4) lead to

$$\|T[P[c]]\|_\infty \le \max_{1\le i\le m}\|T_i[P[c]]\|_\infty \le \max_{1\le i\le m} c_i^\infty e^{\beta|q_i|\|\psi\|_\infty} \le \hat{a}e^{\hat{b}\|c\|_\infty} \le \hat{a}e^{\hat{b}x^*} = x^*.$$

The proof is complete. □

Proof of Proposition 3.1. By (3.10) and Lemma 3.1, it suffices to prove that the sequence $\{c^{(k)}\}$ produced by (B.3) converges. For each $j \ge 1$ we have by the mean-value theorem for operators that

$$\|c^{(j+1)} - c^{(j)}\|_\infty \le \theta_j\|c^{(j)} - c^{(j-1)}\|_\infty,$$

where

$$\theta_j = \|D(T\circ P)(\xi^{(j)})\|_{\mathcal{L}((L^\infty(a,\infty))^m,(L^\infty(a,\infty))^m)} \tag{B.5}$$

with $\xi^{(j)}$ a convex combination of $c^{(j)}$ and $c^{(j+1)}$. Here and below D denotes the Fréchet derivative of the corresponding operators and $\mathcal{L}(X,Y)$ denotes the space of all bounded linear operators from a Banach space X to another Banach space Y. The existence of the Fréchet derivative for the corresponding operator is shown automatically when estimates of the norm of such derivatives are given.

We shall prove below that the assumptions of the proposition imply that there exists a constant θ with $0 < \theta < 1$ such that $\theta_j \le \theta$ for all $j = 1, 2, \dots$. Suppose so, we then have

$$\left\|c^{(j+1)} - c^{(j)}\right\|_\infty \le \theta\left\|c^{(j)} - c^{(j-1)}\right\|_\infty \le \cdots \le \theta^j\left\|c^{(1)} - c^{(0)}\right\|_\infty, \quad j = 1, 2, \dots.$$

Consequently,

$$\begin{aligned}\left\|c^{(k+p)} - c^{(k)}\right\|_\infty &\le \sum_{j=1}^p\left\|c^{(k+j)} - c^{(k+j-1)}\right\|_\infty\\ &\le \left(\sum_{j=1}^p\theta^{k+j-1}\right)\left\|c^{(1)} - c^{(0)}\right\|_\infty\end{aligned}$$

$$\leq \frac{\theta^k}{1-\theta}\left\|c^{(1)}-c^{(0)}\right\|_\infty, \quad k,p=1,2,\ldots.$$

Hence $\{c^{(k)}\}$ is a Cauchy sequence in $(L^\infty(a,\infty))^m$ and thus it converges in $(L^\infty(a,\infty))^m$ to some $c^{(\infty)}$. By (3.10) and Lemma 3.1, $\{\psi^{(k)}\}$ then converges in $L^\infty(a,\infty)$ to some $\psi^{(\infty)}$. Now it follows from (3.10) that $\psi^{(\infty)} = P[c^{(\infty)}]$ and $c^{(\infty)} = T[\psi^{(\infty)}]$ as desired.

We now estimate the norm θ_j. Let $c \in (L^\infty(a,\infty))^m$. By the Chain Rule for Fréchet derivatives, we have

$$\begin{aligned}\|D(T\circ P)[c]\|_{\mathcal{L}((L^\infty(a,\infty))^m,(L^\infty(a,\infty))^m)} &= \|DT[P[c]]\circ DP[c]\|_{\mathcal{L}((L^\infty(a,\infty))^m,(L^\infty(a,\infty))^m)}\\ &\leq \|DT[P[c]]\|_{\mathcal{L}(L^\infty(a,\infty),(L^\infty(a,\infty))^m)}\|DP[c]\|_{\mathcal{L}((L^\infty(a,\infty))^m,L^\infty(a,\infty))}.\end{aligned} \tag{B.6}$$

Recall that

$$\|DP[c]\|_{\mathcal{L}((L^\infty(a,\infty))^m,L^\infty(a,\infty))} = \sup_{0\neq u\in(L^\infty(a,\infty))^m}\frac{\|(DP[c])[u]\|_\infty}{\|u\|_\infty}. \tag{B.7}$$

Let $u = (u_1,\ldots,u_m) \in (L^\infty(a,\infty))^m$. Then $(DP[c])[u] = \frac{\mathrm{d}}{\mathrm{d}t}\big|_{t=0}P[c+tu]$. This is a function of $r > a$. Notice that $P:(L^\infty(a,\infty))^m \to L^\infty(a,\infty)$ is an affine mapping. Denote by $\chi_E(r)$ the characteristic function of a set E, i.e., $\chi_E(r)=1$ if $r\in E$ and $\chi_E(r)=0$ if $r\notin E$. We then obtain from all (3.1), (3.3)–(3.5) and (B.1), and a series of calculations that

$$\begin{aligned}|(DP[c])[u](r)| &= \left|\frac{1}{2\kappa}\int_a^\infty\left[\sum_{i=1}^m\frac{q_i}{\varepsilon_s}u_i(s)\right]\left[\frac{s}{r}\mathrm{e}^{-\kappa(s-r)}+\frac{\mathrm{e}^{2\kappa a}(\kappa a-1)}{\kappa a+1}\frac{s}{r}\mathrm{e}^{-\kappa(s+r)}\right.\right.\\ &\quad\left.\left.-\chi_{(a,r)}(s)\frac{s}{r}\mathrm{e}^{-\kappa(s-r)}+\chi_{(a,r)}(s)\frac{s}{r}\mathrm{e}^{\kappa(s-r)}\right]\right|\mathrm{d}s\\ &\leq\left(\sum_{i=1}^m\frac{|q_i|}{2\kappa\varepsilon_s}\right)\|u\|_\infty\int_a^\infty\left|(1-\chi_{(a,r)})\frac{s}{r}\mathrm{e}^{-\kappa(s-r)}+\frac{\mathrm{e}^{2\kappa a}(\kappa a-1)}{\kappa a+1}\frac{s}{r}\mathrm{e}^{-\kappa(s+r)}+\chi_{(a,r)}(s)\frac{s}{r}\mathrm{e}^{\kappa(s-r)}\right|\mathrm{d}s\\ &\leq\left(\sum_{i=1}^m\frac{|q_i|}{2\kappa\varepsilon_s}\right)\|u\|_\infty\left[\int_r^\infty\frac{s}{r}\mathrm{e}^{-\kappa(s-r)}\mathrm{d}s+\frac{\mathrm{e}^{2\kappa a}|\kappa a-1|}{\kappa a+1}\int_a^\infty\frac{s}{r}\mathrm{e}^{-\kappa(s+r)}\mathrm{d}s+\int_a^r\frac{s}{r}\mathrm{e}^{\kappa(s-r)}\mathrm{d}s\right]\\ &=\left(\sum_{i=1}^m\frac{|q_i|}{\kappa^2\varepsilon_s}\right)\|u\|_\infty\left\{1+\frac{[|\kappa a-1|-(\kappa a-1)]}{2\kappa r}\mathrm{e}^{-\kappa(r-a)}\right\}\\ &\leq\left(\sum_{i=1}^m\frac{|q_i|}{\kappa^2\varepsilon_s}\right)\left[1+\frac{|\kappa a-1|-(\kappa a-1)}{2\kappa a}\right]\|u\|_\infty\quad\forall r>a.\end{aligned}$$

This and (B.7) lead to

$$\|DP[c]\|_{\mathcal{L}((L^\infty(a,\infty))^m,L^\infty(a,\infty))}\leq\left(\sum_{i=1}^m\frac{|q_i|}{\kappa^2\varepsilon_s}\right)\left[1+\frac{|\kappa a-1|-(\kappa a-1)}{2\kappa a}\right]. \tag{B.8}$$

Let now $\psi = P[c]\in L^\infty(a,\infty)$. We estimate

$$\|DT[\psi]\|_{\mathcal{L}(L^\infty(a,\infty),(L^\infty(a,\infty))^m)} = \sup_{0\neq f\in L^\infty(a,\infty)}\frac{\|(DT[\psi])[f]\|_\infty}{\|f\|_\infty}. \tag{B.9}$$

Let $f\in L^\infty(a,\infty)$. We have

$$\begin{aligned}(DT[\psi])[f] &= \frac{\mathrm{d}}{\mathrm{d}t}\bigg|_{t=0}T[\psi+tf]\\ &=\left(\frac{\mathrm{d}}{\mathrm{d}t}\bigg|_{t=0}T_1[\psi+tf],\ldots,\frac{\mathrm{d}}{\mathrm{d}t}\bigg|_{t=0}T_m[\psi+tf]\right)\\ &=(DT_1[\psi][f],\ldots,DT_m[\psi][f]).\end{aligned}$$

Straight forward calculations using the definition of $T_i:L^\infty(a,\infty)\to L^\infty(a,\infty)$ for each i (cf. (3.9)) leads to

$$|DT_i[\psi][f](r)| = \left|\beta q_iT_i[\psi](r)\left[\frac{\int_a^\infty s^{-2}\mathrm{e}^{\beta q_i\psi(s)}f(s)\mathrm{d}s}{\int_a^\infty s^{-2}\mathrm{e}^{\beta q_i\psi(s)}\mathrm{d}s}+f(r)-\frac{\int_a^r s^{-2}\mathrm{e}^{\beta q_i\psi(s)}f(s)\mathrm{d}s}{\int_a^r s^{-2}\mathrm{e}^{\beta q_i\psi(s)}\mathrm{d}s}\right]\right|$$

$$\leq \beta|q_i||T_i[\psi](r)|\left[\left|\frac{\int_a^\infty s^{-2}e^{\beta q_i\psi(s)}f(s)ds}{\int_a^\infty s^{-2}e^{\beta q_i\psi(s)}ds}\right| + |f(r)| + \left|\frac{\int_a^r s^{-2}e^{\beta q_i\psi(s)}f(s)ds}{\int_a^r s^{-2}e^{\beta q_i\psi(s)}ds}\right|\right]$$
$$\leq (3\beta|q_i||T_i[\psi](r)|)\,\|f\|_\infty$$
$$\leq \left(3\beta|q_i|c_i^\infty e^{-q_i\beta\psi(r)}\right)\|f\|_\infty \quad \forall r > a,$$

where in the last step we used the fact that $|T_i[\psi](r)| \leq c_i^\infty e^{-q_i\beta\psi(r)}$ for all $r > a$, which follows from the definition of $T_i : L^\infty(a,\infty) \to L^\infty(a,\infty)$ (cf. (3.9)) and (3.2). Consequently, we have by (B.9) that

$$\|DT[\psi]\|_{\mathcal{L}(L^\infty(a,\infty),(L^\infty(a,\infty))^m)} \leq \max_{1\leq i\leq m}\left(3\beta|q_i|c_i^\infty \sup_{r>a} e^{-q_i\beta\psi(r)}\right).$$

This and (B.4), together with the fact that $\psi = P[c]$, imply

$$\|DT[P[c]]\|_{\mathcal{L}(L^\infty(a,\infty),(L^\infty(a,\infty))^m)} \leq \max_{1\leq i\leq m} 3\beta|q_i|c_i^\infty e^{|q_i|\beta\left[\frac{|Q|a^2}{3\varepsilon_S(\kappa a+1)}+\frac{|\kappa a-1|+2(\kappa a+1)}{2\kappa^3a^2}\sum_{j=1}^m|q_j|(\|c_j\|_\infty+c_j^\infty)\right]}. \tag{B.10}$$

Since ξ_j in (B.5) is a convex combination, we have by Lemma B.1 that

$$\|\xi^{(j)}\|_\infty \leq \max\left(\|c^{(j)}\|_\infty, \|c^{(j+1)}\|_\infty\right) \leq x^*(\hat{a},\hat{b}).$$

Therefore, combining (B.5), (B.6), (B.8) and (B.10), we conclude that

$$\theta_j \leq \hat{A}e^{\hat{B}x^*(\hat{a},\hat{b})} < 1,$$

where $\hat{A}$ and $\hat{B}$ are given by (3.13) and (3.14), respectively. □

References

[1] Z. Radic, D.M. Quinn, J.A. McCammon, P. Taylor, Electrostatic influence on the kinetics of ligand binding to acetylcholinesterase. Distinctions between active center ligands and fasciculin, J. Biol. Chem. 272 (1997) 23265–23277.
[2] F.B. Sheinerman, R. Norel, B. Honig, Electrostatic aspects of protein–protein interactions, Curr. Opin. Struct. Biol. 10 (2000) 153–159.
[3] B.Z. Lu, Y.C. Zhou, G.A. Huber, S.D. Bond, M.J. Holst, J.A. McCammon, Electrodiffusion: A continuum modeling framework for biomolecular systems with realistic spatiotemporal resolution, J. Chem. Phys. 127 (2007) 135102.
[4] J. Che, J. Dzubiella, B. Li, J.A. McCammon, Electrostatic free energy and its variations in implicit solvent models, J. Phys. Chem. B 112 (2008) 3058–3069.
[5] M.E. Davis, J.A. McCammon, Electrostatics in biomolecular structure and dynamics, Chem. Rev. 90 (1990) 509–521.
[6] M. Fixman, The Poisson–Boltzmann equation and its application to polyelecrolytes, J. Chem. Phys. 70 (1979) 4995–5005.
[7] P. Grochowski, J. Trylska, Continuum molecular electrostatics, salt effects and counterion binding—A review of the Poisson–Boltzmann model and its modifications, Biopolymers 89 (2008) 93–113.
[8] B. Li, Continuum electrostatics for ionic solutions with nonuniform ionic sizes, Nonlinearity 22 (2009) 811–833.
[9] B. Li, Minimization of electrostatic free energy and the Poisson–Boltzmann equation for molecular solvation with implicit solvent, SIAM J. Math. Anal. 40 (2009) 2536–2566.
[10] K.A. Sharp, B. Honig, Calculating total electrostatic energies with the nonlinear Poisson–Boltzmann equation, J. Phys. Chem. 94 (1990) 7684–7692.
[11] B.Z. Lu, J.A. McCammon, Kinetics of diffusion-controlled enzymatic reactions with charged substrates, 2009, preprint.
[12] R.S. Eisenberg, Computing the field in proteins and channels, J. Membr. Biol. 150 (1996) 1–25.
[13] M.G. Kurnikova, R.D. Coalson, P. Graf, A. Nitzan, A lattice relaxation algorithm for three-dimensional Poisson–Nernst–Planck theory with application to ion transport through the gramicidin A channel, Biophys. J. 76 (1999) 642–656.
[14] A.E. Cardenas, R.D. Coalson, M.G. Kurnikova, Three-dimensional Poisson–Nernst–Planck theory studies: Influence of membrane electrostatics on gramicidin A channel conductance, Biophys. J. 79 (2000) 80–93.
[15] U. Hollerbach, D.P. Chen, D.D. Busath, R. Eisenberg, Predicting function from structure using the Poisson–Nernst–Planck equations: Sodium current in the gramicidin A channel, Langmuir 16 (2000) 5509–5514.
[16] S. Furini, F. Zerbetto, S. Cavalcanti, Application of the Poisson–Nernst–Planck theory with space-dependent diffusion coefficients to KcsA, Biophys. J. 91 (2006) 3162–3169.
[17] B. Corry, S. Kuyucak, S.H. Chung, Tests of continuum theories as models of ion channels: II. Poisson–Nernst–Planck theory versus Brownian dynamics, Biophys. J. 78 (2000) 2364–2381.
[18] S. Berneche, B. Roux, A microscopic view of ion conduction through the K+ channel, Proc. Natl. Acad. Sci. USA 100 (2003) 8644–8648.
[19] S.Y. Noskov, W. Im, B. Roux, Ion permeation through the α-Hemolysin channel: Theoretical studies based on Brownian dynamics and Poisson–Nernst–Planck electrodiffusion theory, Biophys. J. 87 (2004) 2299–2309.
[20] B. Roux, T. Allen, S. Berneche, W. Im, Theoretical and computational models of ion channels, Q. Rev. Biophys. 37 (2004) 15–103.
[21] C.L. Lopreore, T.M. Bartol, J.S. Coggan, D.X. Keller, G.E. Sosinsky, M.H. Ellisman, T.J. Sejnowski, Computational modeling of three-dimensional electrodiffusion in biological systems: Application to the node of ranvier, Biophys. J. 95 (2008) 2624–2635.
[22] H. Qian, J.A. Schellman, Transformed Poisson–Boltzmann relations and ionic distributions, J. Phys. Chem. B 104 (2000) 11528–11540.